Arabidopsis transcript and metabolite profiles: ecotype-specific responses to open-air elevated [CO₂]

PINGHUA LI[1]*, ELIZABETH A. AINSWORTH[1,4], ANDREW D. B. LEAKEY[1,3], ALEXANDER ULANOV[2], VERA LOZOVAYA[2], DONALD R. ORT[1,3,4] & HANS J. BOHNERT[1,2,3]

[1]*Department of Plant Biology,* [2]*Department of Crop Sciences,* [3]*Institute for Genomic Biology, University of Illinois at Urbana-Champaign, Urbana, IL 61801, USA and* [4]*Photosynthesis Research Unit, USDA-ARS, Urbana, IL 61801, USA*

ABSTRACT

A Free-Air CO₂ Enrichment (FACE) experiment compared the physiological parameters, transcript and metabolite profiles of *Arabidopsis thaliana* Columbia-0 (Col-0) and Cape Verde Island (Cvi-0) at ambient (~0.375 mg g⁻¹) and elevated (~0.550 mg g⁻¹) CO₂ ([CO₂]). Photoassimilate pool sizes were enhanced in high [CO₂] in an ecotype-specific manner. Short-term growth at elevated [CO₂] stimulated carbon gain irrespective of down-regulation of plastid functions and altered expression of genes involved in nitrogen metabolism resembling patterns observed under N-deficiency. The study confirmed well-known characteristics, but the use of a time course, ecotypic genetic differences, metabolite analysis and the focus on clusters of functional categories provided new aspects about responses to elevated [CO₂]. Longer-term Cvi-0 responded by down-regulating functions favouring carbon accumulation, and both ecotypes showed altered expression of genes for defence, redox control, transport, signalling, transcription and chromatin remodelling. Overall, carbon fixation with a smaller commitment of resources in elevated [CO₂] appeared beneficial, with the extra C only partially utilized possibly due to disturbance of the C : N ratio. To different degrees, both ecotypes perceived elevated [CO₂] as a metabolic perturbation that necessitated increased functions consuming or storing photoassimilate, with Cvi-0 emerging as more capable of acclimating. Elevated [CO₂] in *Arabidopsis* favoured adjustments in reactive oxygen species (ROS) homeostasis and signalling that defined genotypic markers.

Key-words: *Arabidopsis* ecotypes; elevated CO₂; FACE; metabolite profiling; transcript profiling.

INTRODUCTION

Projections about global atmospheric [CO₂] assume an increase to ~0.550 mg g⁻¹ by 2050 (Prentice *et al.* 2001), which may be expected to lead to significant beneficial

Correspondence: H. J. Bohnert. Fax: +1 217 333 5574; e-mail: bohnerth@life.uiuc.edu

*Present address: Department of Molecular Biology and Genetics, Cornell University, 317 Biotechnology Building, Ithaca, NY 14853, USA

impact on plants in managed and natural ecosystems. C₃ plants can respond to elevated [CO₂] with increased photosynthesis, growth and productivity as well as reduced stomatal conductance (g_s), promoting not only lower transpiration but also possibly less evaporative cooling (see Ainsworth & Rogers 2007 for a review). While photosynthesis (A) is generally increased in C₃ plants at elevated [CO₂], the down-regulation of photosynthesis in elevated [CO₂], including reduced ribulose 1·5-bisphosphate carboxylase/oxygenase (Rubisco) content and maximum apparent carboxylation capacity ($V_{c,max}$), may affect metabolic homeostasis, which could then constrain the overall stimulation of carbon fixation (Cheng, Moore & Seemann 1998; Ainsworth *et al.* 2007). At elevated [CO₂], decreases in Rubisco and overall N-content are associated with increases in sugars and starch, and increased concentrations of secondary metabolites and structural components (Ludewig *et al.* 1998; Peñuelas & Estiarte 1998; Castells *et al.* 2002). However, significant variation exists at the level of physiological responsiveness and the magnitude of increases in productivity to elevated [CO₂] across species and ecotypes (Bazzaz *et al.* 1995; Long *et al.* 2004; Ainsworth *et al.* 2007). How such intra- and interspecific physiological plasticity is grounded in genetic organization and molecular regulation is largely unknown.

Molecular bases for responses to elevated [CO₂] have been measured in poplar trees grown in the field (Gupta *et al.* 2005; Taylor *et al.* 2005). After long-term exposure to elevated [CO₂], transcript abundance differences were dependent on leaf developmental age. Transcripts that showed differences in the comparison of ambient versus elevated [CO₂] included many chloroplast-related functions as down-regulated, while functions associated with development, defence and signalling showed increased expression (Gupta *et al.* 2005; Taylor *et al.* 2005). Effects of elevated [CO₂] on gene expression in FACE-grown soybeans contrasted growing and mature leaves (Ainsworth *et al.* 2006). Apart from differences that revealed developmental stage differences, such as the machineries required to promote the growth of cells, the analysis identified ([CO₂] × development) interactions. Elevated [CO₂] stimulated cell growth and differentiation in young leaves compared with leaves in ambient air. The [CO₂]-specific portion of the transcript profile indicated increased conduits directing

carbohydrates into respiratory pathways for energy-producing and anabolic reactions. A recent study that focused on amino acids (Ainsworth *et al.* 2007) reported [CO_2]-dependent disturbances in amino acids, with the disturbance of the Glu/Gln ratio persisting independent of leaf age and time.

To harness the evolutionary diversity of *Arabidopsis thaliana* (Duarte *et al.* 2006) and make use of the tools available for this species, mature, pre-flowering *Arabidopsis* ecotypes were exposed to ambient and elevated [CO_2] to determine how fast and to what extent the lines acclimated to the rapid change in carbon availability. We used field-grown plants (http://www.soyface.uiuc.edu), where the rapid growth of the plants, high rates of photosynthesis and enhanced carbohydrate metabolism were measured in the background of normal abiotic and biotic stress conditions (Miyazaki *et al.* 2004).

From a collection of *Arabidopsis* ecotypes, Columbia-0 (Col-0) and Cape Verde Island (Cvi-0) were selected based on their performance and evolutionary history. Adapted to different environments, they showed different physiological responses in elevated [CO_2] in the field (Li *et al.* 2006). Expanding on earlier observations, transcript and metabolite profiles were recorded at two time points of growth in FACE. The two ecotypes responded differently to elevated [CO_2], with Cvi-0 experiencing less metabolic perturbation, apparently adapting to changes faster than Col-0. The transcript and metabolite profiles alike indicated a disturbance of nitrogen metabolism in the background of high carbon gains, which might have affected the C : N sensing early during the growth of the plants in the field.

MATERIALS AND METHODS

Plant material and CO_2 exposure

Arabidopsis thaliana ecotypes Col-0 and Cvi-0 plants were germinated and grown in fertilized soil in $0.5 \times 0.2 \times 0.3$ m trays in a growth room (150 μmol m^{-2} s^{-1}, 24 °C) until they reached the early rosette stage (3 weeks). After 5 d in a greenhouse, the plants were transferred to the SoyFACE facility (http://www.soyface.uiuc.edu; Miyazaki *et al.* 2004; Li *et al.* 2006). The plants in three plots (ambient air) experienced current [CO_2] of 0.375 mg g^{-1}, while the plants in three CO_2 plots (elevated CO_2) were treated with [CO_2] of 0.550 mg g^{-1}, simulating the expected environment in 2050. Weather reports accompanying the entire experiment can be found at http://www.soyface. uiuc.edu/weather.htm.

Plants of a comparable developmental stage used for microarray and metabolite analyses were harvested in 21 and 27 June at 9:00–10:00 am. Aboveground material was collected from 10 plants (as a pool) in each ring, immediately frozen in N$_2$, and stored at −80 °C for both RNA extraction and metabolites assay. The climatic conditions for the 24 h time period before harvest and during harvest are provided in Supporting Information Table S1.

Physiological parameters

Pre-dawn 14 June, immediately prior to transfer from the glasshouse to the field, the maximum, dark-adapted quantum yield of photosystem II (PSII) (F_v/F_m) of fully expanded leaves was measured using a pulse-modulated chlorophyll fluorescence system (FMS2; Hansatech Instruments, King's Lynn, Norfolk, UK). Measurements were repeated in the field pre-dawn in 15, 17 and 19 June. Net photosynthetic CO_2 assimilation (*A*), stomatal conductance (g_s) and intercellular leaf [CO_2] (c_i) were measured with a standard gas exchange system with 1 cm^2 leaf chamber (LI-6400 and LI-6400-40; Li-Cor, Inc., Lincoln, NE, USA) on 19 June between 11:00 and 14:00 h with ambient conditions of photosynthetic photon flux density (PPFD) (1250 μmol m^{-2} s^{-1}), air temperature (27 °C), relative humidity (RH) ($\geq$65%) and treatment [CO_2] [375 μmol m^{-2} s^{-1} (ambient), 550 μmol m^{-2} s^{-1} (elevated)]. External halogen light was used for constant illumination during gas exchange measurements.

In 21 and 27 June, leaves were sampled for chlorophyll, protein and starch determination with standard methods (Porra, Thompson & Kriedemann 1989; Stitt *et al.* 1989). Five replicates were taken from each experimental plot (*n* = 3). Dried leaf material was powdered and analysed for N content using an elemental combustion system (Model 4010; Costech Analytical, Inc., Valencia, CA, USA).

RNA extraction, microarray hybridizations and microarray data analysis

Total RNA from two ambient plots and two elevated [CO_2] plots (as two biological repeats) was isolated (CTAB method; Jaakola *et al.* 2001) from the pooled plants. Purified RNAs (60 μg each, Qiagen RNeasy kit; Qiagen, Carlsbad, CA, USA) from ambient and elevated [CO_2] were reverse transcribed (SuperScript III; Invitrogen, Carlsbad, CA, USA), and cDNAs were labelled with Cy3 or Cy5 by indirect labelling (Miyazaki *et al.* 2004; Li *et al.* 2006). Microarray slides with >26 000 DNA elements (70-mer gene-specific oligonucleotides; Qiagen/Operon, Valencia, CA, USA) were used (http://www.ag.arizona.edu/ microarray) (Miyazaki *et al.* 2004; Gong *et al.* 2005; Li *et al.* 2006). To avoid bias in microarrays as a consequence of dye-related differences in labelling efficiency, dye labelling for each paired sample (elevated CO_2/ambient CO_2) was swapped (for details, see the Supporting Information text).

After hybridization, the slides were scanned (GENEPIX 4000B; Axon Instruments, Union City, CA, USA), and spot intensities were extracted (GENEPIX PRO 6.0). Spots with intensities lower than the background or with an aberrant spot shape were flagged by GENEPIX software and were checked manually.

Filtered raw intensity data sets were then analysed using the R/MAANOVA microarray analysis program (http://research.jax.org/faculty/churchill/software/Rmaanova v.1.8.1). We smoothed the data with the spatial-intensity joint lowess, and then fitted the data into a mixed-model

analysis of variance (ANOVA) in two stages (normalization modelling followed by gene-specific effect modelling) with [CO₂] treatment, ecotype and dye as fixed effects, and array and sample as random effects. Analyses were based on Fs statistics, a modified F statistics incorporating James–Stein shrinkage estimates of variance components (Cui *et al.* 2005). Significant changes in expression between elevated [CO₂] and ambient [CO₂] were determined by calculating the P-values for the Fs statistics using 100 random permutations with fold changes of at least of 1.3. The P-values were adjusted to correct for type I error with the FDR correction implemented in R/MAANOVA. Cut-off adjusted P-values were 0.05. Because there were no direct hybridization experiments performed between ecotypes, ecotype-specific genes were picked up by MAANOVA at a more stringent level, with an FDR-adjusted $P < 0.05$ and a fold change cut-off of 3.

MapMan visualization

Microarray data (log₂ fold change of elevated [CO₂] versus ambient air) were imported into MapMan (http://gabi.rzpd.de/projects/MapMan/ v. 1.5.0, Thimm *et al.* 2004), converted to a false colour scale, and used for pathway and/or functional category analysis. Wilcoxon rank-sum test was used to predict categories that exhibited a different behaviour in terms of their expression profile compared with all other remaining categories. Benjamini and Hochberg false discovery rate control procedure was used to correct the P-values.

Real-time PCR

To verify hybridization results, real-time PCR using SYBR-green (Applied Biosystems, Forster City, CA, USA) and ABI PRISM/Taqman 7900 Sequence Detection System (Applied Biosystems) was conducted as described (Li *et al.* 2006). One microgram of RNA from each condition was used for first-strand cDNA synthesis, and the internal control was actin-3 (Supporting Information Table S2 for primer sequences). Four repeats were carried out for each gene, and averaged threshold cycle numbers were used to calculate changes (log₂).

Metabolite profiling

Same pools of plant material used for RNA extraction were dried under N₂. Methanol extracts were obtained and derived according to Roessner *et al.* (2000). Samples of 1–2 μL were injected with a split ratio of 8:1. The gas chromatography-mass spectrometry (GC-MS) system consisted of an HP5890 gas chromatograph and an HP5970 mass selective detector (Agilent, Inc., Palo Alto, CA, USA) and an Rtx-1701 (30 m × 0.25 mm i.d., 0.25 μm film thickness) capillary column (Restek, Bellefonte, PA, USA). Data from three independent replicates were normalized to the internal standard (hentriacontanoic acid; 10 mg mL⁻¹). Chromatograms were evaluated as described (Lozovaya *et al.* 2006).

Methanol : water extracts were dried and extracted with 0.1 M HCl (3 × 1 mL) at room temperature, and were centrifuged for 10 min at 20 000 *g*. Supernatants were collected, filtered, purified and derived according to Silva *et al.* (2003). Samples were dried under N₂ and were stored at –20 °C prior to derivation. For GC-MS analysis, both injector and detector were at 250 °C. Helium carrier gas flow rate was 1 mL min⁻¹ with a temperature programme from 100 (1 min isothermal heating; solvent delay = 3 min) to 280 °C at 20 °C min⁻¹ and 280 °C for 5 min, and mass spectra were recorded in the m/z 50–300 range. Peaks were compared with an electron impact mass spectrum library containing standard spectra of ethylchloroformate (ECF) derivatives and normalized to the internal standard (L-*p*-chlorophenylalanine; mg mL⁻¹) for comparison among samples. The chromatograms and mass spectra were evaluated using HP Chemstation (Agilent, Palo Alto, CA, USA) and AMDIS (NIST, Gaithersburg, MD, USA) programs.

Statistical analysis of metabolites

All data from three biological replicates per sample were statistically analysed by *t*-test and one-way ANOVA using the algorithm incorporated into Microsoft Excel 2002 (Microsoft Corporation, Seattle, WA, USA). Multivariate statistical analysis was performed using principal component analysis (PCA) (Jobson 1992; Jolliffe 2002) implemented in XLSTAT-2007 (Addinsoft, New York, NY, USA). Significance is defined for changes statistically significant at $P < 0.05$.

RESULTS

Environmental conditions

After transplanting greenhouse-grown, pre-flowering rosettes (14 June), the plants were sampled on 21 and 27 June 2005. The climatic conditions differed on days preceding the harvest dates (Supporting Information Table S1A) with average temperatures of 26.4 (21 June) and 30.4 °C (27 June), 52–53% RH on both days, and 1650+/− 10 μmol photons m⁻² s⁻¹, respectively, at both harvest times (0900–1000 h). By 27 June, both ecotypes had begun to flower irrespective of their location either in elevated [CO₂] or in ambient conditions.

Leaf gas exchange, chlorophyll fluorescence, soluble protein, chlorophyll and starch contents during exposure to elevated [CO₂]

The maximum quantum yield of PSII (F_v/F_m), measured pre-dawn immediately before the plants were taken to the field (14 June), was ~0.80 for both ecotypes (Fig. 1a). F_v/F_m decreased upon exposure to field conditions (15 June), but recovered to pre-transfer levels within 3–4 d in the field, suggesting that the plants overcame the initial stress imposed by exposure to the field. Growth at ambient versus elevated [CO₂] had no effect on the F_v/F_m response. Under
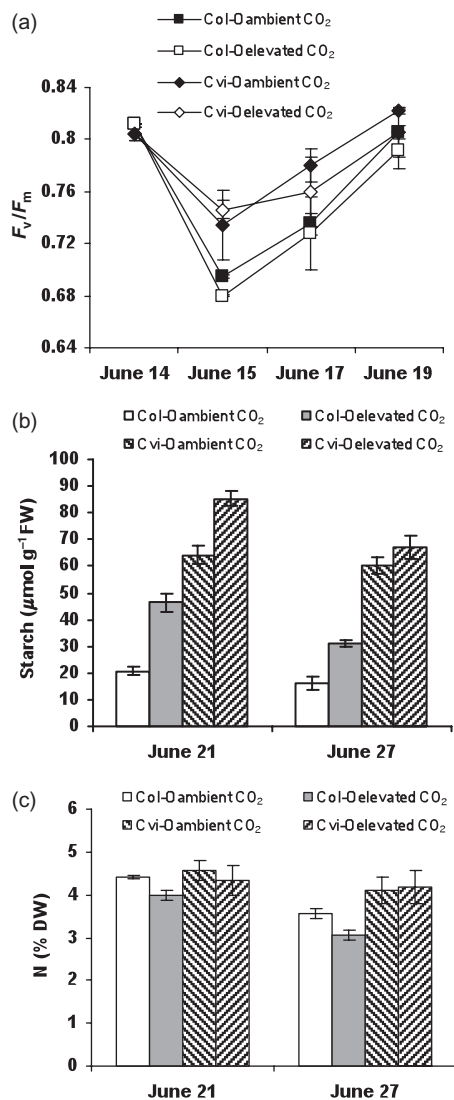
Figure 1. Physiological parameters of *Arabidopsis* ecotypes in elevated $[CO_2]$. The data represent the mean ($\pm$SD) from three rings (5 repeats per ring, and 10 plants pooled in each ring). (a) Maximum quantum yield of photosystem II (F_v/F_m) measured before and after transfer into the field; (b) starch content; (c) nitrogen content.

ambient conditions, Cvi-0 exhibited higher rates of photosynthesis (A) and stomatal conductance (g_s) than Col-0. Significant stimulation of A was observed in elevated $[CO_2]$ with rates for both ecotypes roughly double than those in ambient air (Table 1). Under elevated $[CO_2]$, g_s changed only in Col-0, and C_i increased in both ecotypes (Table 1). There was no effect of elevated $[CO_2]$ on chlorophyll or total soluble protein in 21 June, but decreases were significant in 27 June in both ecotypes (Supporting Information Fig. S1), and no effect was observed by elevated $[CO_2]$ or ecotype on the fresh weight to dry weight ratio (data not shown). The effect of elevated $[CO_2]$ on starch content varied between ecotypes (Fig. 1b). Cvi-0 accumulated approximately twice the amount of starch compared with

Col-0 in ambient air. In 21 June, starch content increased under elevated $[CO_2]$ in Col-0 (130%) and Cvi-0 (25%), but by 27 June, starch increases were less pronounced (Col-0) or barely detectable (Cvi-0). Figure 1c shows the N content (% dry weight) of the plant material used for microarray analyses. There was no effect of elevated $[CO_2]$ on N in Cvi-0, but Col-0 showed a slightly reduced N after exposure to elevated $[CO_2]$ at both time points.

Transcript profiles

Gene expression was affected by $[CO_2]$ treatment, ecotype and sampling date. Hierarchical clustering revealed a correlation between harvest date and the behaviour of the transcriptome at the two time points, which clustered separately (Supporting Information Fig. S2). Furthermore, when calculating the Pearson correlation coefficients of the transcriptome for the 21 and 27 June harvest dates in both ecotypes, no significant relationship emerged within each ecotype harvested at different dates, but high correlation existed between ecotypes harvested at the same time (Supporting Information Table S1B). The high degree of correspondence between harvest date and transcript profiles of Col-0 and Cvi-0 in response to elevated $[CO_2]$ reflects a strong dependence on daily fluctuations in temperature or other climatic factors, and presumably also on the developmental state. Indeed, the plants experienced different conditions at the two harvest dates (Supporting Information Table S1A). Further, we first describe transcripts with significant responses to elevated $[CO_2]$ determined by mixed-model ANOVA for both ecotypes, on the first and second harvest dates, respectively. We then describe changes in gene expression, which differ between ecotypes. Genes for validation of microarray hybridizations by qRT-PCR in the ecotypes were also selected. The results are represented as the difference in threshold numbers between ambient and elevated $[CO_2]$ after primers had been tested for amplification in a linear range (Supporting Information Table S2; Supporting Information Fig. S3). Correlation was high overall, while absolute fold changes diverged between the two methods.

The first harvest date

Ecotypes harvested at the same date showed high correlation in their gene expression profiles. Mixed-model ANOVA

Table 1. Photosynthetic gas exchange parameters

Ecotype	CO_2	A	g_s	C_i
Col-0	Ambient	6.6 ± 0.9	0.20 ± 0.02	0.320 ± 0.013
	Elevated	11.7 ± 0.7	0.14 ± 0.02	0.393 ± 0.027
Cvi-0	Ambient	11.1 ± 2.2	0.26 ± 0.10	0.297 ± 0.013
	Elevated	20.7 ± 2.2	0.31 ± 0.07	0.394 ± 0.052

A, light-saturated CO_2 assimilation; g_s, stomatal CO_2 conductance; C_i, intercellular $[CO_2]$ (mg g^{-1}) (recorded 19 June 2005).

was applied to investigate similar regulatory trends in transcript complexity in response to [CO$_2$] across the ecotypes. In 21 June, the [CO$_2$] response indicated 215 transcripts down-regulated and 296 up-regulated in both ecotypes at a fold change of at least 1.3 (FDR-adjusted $P < 0.05$) (Supporting Information Table S3A,B). A significant down-regulation was observed in both ecotypes in genes related to photosynthesis including light reaction functions, the Calvin cycle and photorespiration (Table 2, Supporting Information Table S3A). Transcripts for the photosystem (PSI and II) subunits, *PsaK*, *PsaN*, *PsbQ*, *PsbW*, *PsbX* and *PsbO2*, encoding proteins of the PSI/II core, assembly and stability, were reduced most significantly. Decreased expression of transcripts for light-harvesting and electron transport-related proteins was also evident. Glyceraldehyde-3-phosphate dehydrogenase (*GAPA*), whose products are known to interact with CP12 proteins *in vivo* in the Calvin cycle, was coordinately down-regulated along with *CP12-1* and *CP12-2*. Chlororespiratory reduction 7 (CRR7), encoding a protein of the plastid NAD(P)H dehydrogenase complex involved in chlororespiration, photosystem I (PSI) cyclic electron transport and [CO$_2$] uptake, and glycine decarboxylase complex H (GDCH) transcript involved in photorespiration were also significantly down-regulated. Chloroplast development and lipid composition were affected, with *ACP4* (biosynthesis of fatty acids for chloroplast membrane structure) and *FAD5* (related to thylakoid lipid composition) significantly down-regulated. Overall, genes that centred on chloroplast functions were down-regulated irrespective of the physiological data that showed increased carbon assimilation and starch accumulation in elevated [CO$_2$] (Fig. 1b).

Up-regulated genes emphasized functions in transcripts related to C metabolism and utilization (Table 2, Supporting Information Table S3B). Highly expressed genes encoded precursors for functions related to cell walls (*UGD*, *UXS* and *RHM1*), cellulose synthesis enzymes (*CESA* and *CSLC*) and cell wall proteins (arabinogalactan-protein and proline-rich extensin), indicating an active allocation of C to cell walls and also consistent with starch accumulation by both ecotypes (21 June). Equally up-regulated were transcripts for a number of genes with a function in glycolysis and organic acid [tricarboxylic acid cycle (TCA) cycle] metabolism including cytosolic phosphoenolpyruvate (PEP)-carboxylase, oxoglutarate decarboxylase and two ATP-citrate synthases (*ACLB1, 2*). Trehalose phosphate synthase (*TPS*) and trehalose-6-phosphate phosphatase (*TPP*), involved in trehalose metabolism, *ATGSL12* involved in callose biosynthesis, and fructokinase involved in starch/sucrose degradation were induced by elevated [CO$_2$].

Up-regulated transcripts in the category secondary metabolism identified functions in the synthesis of anthocyanins, lignin and flavonoids, exemplified by PAP1, *LDOX*, *PAL1* and *DER*. Transport-associated transcripts that increased included sugar-phosphate transporters (glucose-6-phosphate/phosphate translocator) and amino acid transporter (*AAP2*). Interestingly, many members in the category

vesicle transport were also highly induced in elevated [CO$_2$]. The increase of transcripts encoding disease resistance proteins, HSPs and dehydration-responsive proteins also indicated an active plant response to the environment, which was slightly enhanced in elevated [CO$_2$]. For the regulated transcripts, protein localization was determined as predicted by TargetP (>0.7) and Gene Ontology (GO). In 21 June, most down-regulated genes identified plastid-localized proteins, while up-regulated genes specified transcripts for components of the endomembrane system (Table 2, Supporting Information Table S3).

The second harvest date

Eighty down-regulated and 232 up-regulated transcripts responded to elevated [CO$_2$] in both ecotypes on the second harvest date (27 June; Supporting Information Table S3C,D). At this time point, most transcripts for proteins associated with endomembranes were down-regulated, while the number of functions related to mitochondria increased slightly (TargetP [>0.7] and GO; Table 2, Supporting Information Table S3).

Many genes involved in carbon utilization showed down-regulation at the second harvest date in plants grown in elevated [CO$_2$], for example, *ATCSLC08*, possibly a sign that the plants entered senescence. Genes in the category secondary metabolism, especially in the flavonoids biosynthetic pathway, were also down-regulated in elevated [CO$_2$]. Unexpectedly, many histone gene transcripts were down-regulated in both ecotypes, possibly indicating changes in chromatin structure (Table 2, Supporting Information Table S3C).

A preponderance of transcripts in categories of stress/defence was up-regulated in 27 June (Table 2, Supporting Information Table S3D). A number of heat-shock proteins were outstanding, as well as glutathione S-transferases (GSTs), peroxidases, involved in redox scavenging, heat and drought tolerance. Galactinol synthases (*GOLS1&2*) also was greatly up-regulated in elevated CO$_2$, indicating an active metabolism related to raffinose biosynthesis and metabolism.

Ecotype-specific genes

Mixed-model ANOVA based on Fs statistics was applied to identify differentially expressed genes that distinguished ecotypes. Considering that the plants at the two harvest dates represented different developmental stages and experienced different temperature conditions, the two time points were analysed separately. In the absence of direct hybridizations between ecotypes, statistical analysis (FDR adjusted to $P < 0.05$) with a fold-change cut-off of 3 was taken. In total, 77 genes (21 June) and 215 genes (27 June) showed at least a threefold higher expression in Cvi-0 than in Col-0 (Table 3, Supporting Information Table S4). In contrast, 66 (21) and 156 (27 June) transcripts showed a higher expression in Col-0 compared with Cvi-0 (Table 3, Supporting Information Table S4).

Table 2. Selected genes that differentially expressed between ambient CO_2 and elevated CO_2 (adjusted $P < 0.05$)

AGI	Short description	Col-0 log$_2$(E/A)	Cvi-0 log$_2$(E/A)	Localization
21 June down				
Photosynthesis				
At1g12900	GAPA-2 (glyceraldehyde-3-phosphate dehydrogenase)	−0.46	−0.50	Chloroplast
At1g19150	LHCA6 (photosystem I light harvesting complex gene 6)	−0.73	−0.70	Chloroplast
At1g30380	PSAK (photosystem I subunit K)	−0.57	−0.51	Chloroplast
At1g60950	FED A (ferredoxin 2)	−0.41	−0.42	Chloroplast
At2g06520	PSBX (photosystem II subunit X)	−0.50	−0.54	Chloroplast
At2g26500	Cytochrome b6f complex subunit (petM)	−0.55	−0.46	Chloroplast
At2g34430	LHB1B1 (photosystem II light-harvesting complex gene 1.4	−0.79	−0.56	Chloroplast
At2g35370	GDCH (glycine decarboxylase complex H)	−0.51	−0.66	Mitochondrion
At2g47400	CP12-1 (CP12 domain-containing protein 1)	−0.56	−0.41	Chloroplast
At3g27690	LHCB2:4 (photosystem II light-harvesting complex gene 2.3)	−0.50	−0.54	Chloroplast
At3g50820	PSBO-2	−0.57	−0.59	Chloroplast
At3g62410	CP12-2	−0.55	−0.58	Chloroplast
At4g21280	PSBQ	−0.59	−0.61	Chloroplast
At4g28660	PSB28 (photosystem II reaction centre W family protein)	−0.91	−0.56	Chloroplast
Defence/redox				
At2g25080	ATGPX1 (glutathione peroxidase)	−0.64	−0.56	Chloroplast
At4g25100	FSD1 (iron superoxide dismutase)	−0.79	−0.63	Chloroplast
21 June up				
Amino acid metabolism				
At2g36880	ATBCAT-2 (branched-chain-amino-acid transaminase)	0.75	0.68	Chloroplast
At3g03780	ATMS2 (methionine synthase 2)	0.55	0.69	Cytosol
At3g16150	L-asparaginase, putative	0.75	0.43	–
At5g49810	MMT (methionine S-methyltransferase)	0.49	0.59	–
Carbon metabolism				
At1g53310	Phosphoenolpyruvate carboxylase	0.42	0.46	Cytosol
At3g06650	ACLB-1 (ATP-citrate lyase B-1)	0.39	0.46	Cytosol
At3g55410	2-Oxoglutarate dehydrogenase E1 component, putative	0.41	0.47	Mitochondrion
At4g17770	ATTPS5 (trehalose phosphatase/synthase 5)	0.53	0.47	–
At4g22590	Trehalose-6-phosphate phosphatase	0.75	0.40	Chloroplast
At5g49460	ACLB-2 (ATP-citrate lyase B-2)	0.68	0.52	Cytosol
At5g65690	PEPCK	0.48	0.42	–
Cell wall				
At1g76930	ATEXT4 (extensin 4)	0.75	0.87	Secretory
At2g37090	IRX9 (irregular xylem 9)	1.04	0.68	Secretory
At3g29360	UDP-glucose 6-dehydrogenase, putative	0.61	0.47	Secretory
At3g46440	UXS5 (UDP-Xyl synthase 5)	0.54	0.61	Chloroplast
At3g54590	ATHRGP1 (hydroxyproline-rich glycoprotein)	0.79	1.26	Secretory
At4g18780	CESA8 (cellulose synthase)	1.10	0.72	Secretory
At4g39350	CESA2 (cellulose synthase)	0.66	0.51	Secretory
At5g05170	CESA3 (cellulose synthase)	0.50	0.45	Secretory
At5g64740	CESA6 (cellulose synthase)	0.47	0.46	Secretory
Defence/redox				
At1g32230	RCD1 (radical-induced death 1)	0.42	0.51	Nucleus
At4g10250	HSP22.0	0.79	0.76	Secretory
At4g27670	HSP21	1.36	0.65	Chloroplast
At5g17220	ATGSTF12 (glutathione transferase)	0.61	0.82	Cytoplasm
Secondary metabolism				
At2g37040	PAL1 (phenylalanine ammonia-lyase)	0.57	0.57	cytoplasm
At2g38080	IRX12/LAC4 (laccase 4)	0.87	0.62	Secretory
At4g22870	Anthocyanidin synthase	0.81	1.49	–
At4g22880	LDOX (tannin-deficient seed 4)	0.75	1.21	–
At5g07990	TT7 (flavonoid 3′-monooxygenase)	0.41	0.54	Mitochondrion
Transport				
At2g21390	Coatomer subunit alpha, putative	0.69	0.63	Mitochondrion
At2g34660	ATMRP2 (ATPase)	0.49	0.53	Secretory
At3g16340	ATPDR1/PDR1 (ATPase)	0.52	0.53	Chloroplast
At4g03950	Glucose-6-phosphate/phosphate translocator	0.83	1.09	Secretory
At4g31480	Coatomer beta subunit, putative	0.42	0.58	Secretory
At4g31490	Coatomer beta subunit, putative	0.41	0.47	Secretory
At4g32640	sec23/sec24 transport protein	0.47	0.55	Secretory
At5g09220	AAP2 (amino acid permease)	0.53	0.40	Secretory
27 June down				

Table 2. *Continued*

AGI	Short description	Col-0 log$_2$(E/A)	Cvi-0 log$_2$(E/A)	Localization
Cell wall				
At2g20870	Cell wall protein precursor, putative	−1.50	−0.84	Secretory
At2g24630	ATCSLC08 (Cellulose synthase-like C8)	−0.88	−0.51	Secretory
At3g62680	PRP3 (proline-rich protein)	−0.99	−1.46	Secretory
DNA metabolism/chromatin structure				
At3g53730	Histone H4	−0.40	−0.41	Nucleus
At5g10980	Histone 3.3	−0.43	−0.38	Nucleus
Secondary metabolism				
At3g55120	TT5 (chalcone isomerase)	−0.65	−0.40	Secretory
At5g07990	TT7 (flavonoid 3′-monooxygenase)	−0.53	−0.64	Mitochondrion
At5g08640	FLS (flavonol synthase)	−1.08	−0.73	–
At5g13930	CHS (naringenin-chalcone synthase)	−0.85	−0.55	Secretory
27 June up				
Carbon metabolism				
At1g56600	ATGOLS2 (galactinol synthase)	0.48	0.75	–
At2g36460	Fructose-bisphosphate aldolase, putative	0.58	0.53	Mitochondrion
At2g36850	ATGSL08 (1,3-beta-glucan synthase)	0.50	0.47	Secretory
At2g47180	ATGOLS1 (galactinol synthase)	0.83	0.80	–
At5g04120	Phosphoglycerate/bisphosphoglycerate mutase family protein	0.43	0.44	–
Defence/redox				
At2g29490	ATGSTU1 (glutathione transferase)	0.75	0.59	Cytoplasm
At2g29480	ATGSTU2	1.31	0.57	Cytoplasm
At2g29460	ATGSTU4	0.54	0.53	Cytoplasm
At2g29440	ATGSTU6	0.90	0.58	Cytoplasm
At5g62480	ATGSTU9	0.78	0.55	Cytoplasm
At1g78380	ATGSTU19	0.72	0.52	Cytoplasm
At1g17180	ATGSTU25	0.80	0.54	Cytoplasm
At3g09640	APX2 (ascorbate peroxidase)	1.38	0.99	Cytoplasm
At1g16030	HSP70B	1.61	1.46	Cytoplasm
At1g52560	HSP26.5-P	2.46	0.93	Mitochondrion
At1g54050	HSP17.4-CIII	1.29	1.68	Chloroplast
At1g59860	HSP17.6A	1.51	1.42	Cytosol
At1g74310	HSP101	1.00	1.33	–
At2g25140	HSP98.7	1.01	1.05	Mitochondrion
At2g26150	ATHSFA2	0.48	1.11	Nucleus
At2g29500	HSP17.6B-CI	1.12	1.27	–
At2g32120	HSP70T-2	1.48	1.21	–
At3g44110	ATJ3 (DnaJ homolog 3)	0.55	0.66	–
At3g51910	HSFA7A	1.44	1.89	Nucleus
At4g21320	HSA32	1.29	0.88	–
At4g25200	HSP23.6-M	1.33	1.05	Mitochondrion
At4g36990	HSF4	0.87	0.70	Nucleus
At5g05410	DREB2A	0.55	1.14	Nucleus
At5g12020	HSP17.6-CII	1.18	1.23	–
At5g12030	HSP17.6A	1.35	1.22	Cytoplasm
At5g22060	ATJ2 (DnaJ homolog 2)	0.51	0.51	–
At5g51440	HSP23.5-M	1.28	1.30	Mitochondrion
At5g52640	HSP81-1	0.78	0.96	–
At5g56000	HSP81-4	0.53	0.90	Secretory
Lipid metabolism				
At1g71160	Beta-ketoacyl-CoA synthase family protein	0.65	0.86	Secretory
At1g75960	AMP-binding protein, putative	0.86	0.62	–
At3g03310	Lecithin : cholesterol acyltransferase family protein	0.49	0.56	–
Transport				
At1g30220	ATINT2 (INOSITOL TRANSPORTER 2)	0.76	1.06	Secretory
At1g51340	MATE efflux family protein	0.44	0.58	Secretory
At1g70300	KUP6 (K+ uptake permease 6)	0.47	0.57	Secretory
At2g37180	RD28 (plasma membrane intrinsic protein 2;3)	0.43	0.42	Secretory
At4g28390	AAC3 (ATP : ADP antiporter)	0.64	0.54	Mitochondrion
At1g30220	ATINT2 (INOSITOL TRANSPORTER 2)	0.76	1.06	Secretory
At1g51340	MATE efflux family protein	0.44	0.58	Secretory

The entire gene list is provided in Supporting Information Table S3.

AGI, Arabidopsis Genome Initiative.

Table 3. Selected genes that differentially expressed between Col-0 and Cvi-0 (adjusted *P* < 0.05)

AGI	Category	Short description	21 June (Cvi/Col)	27 June (Cvi/Col)
At4g15260	Carbon metabolism	UDP-glucosyl transferase	6.34	4.22
At1g74590	Defence/redox	ATGSTU10	5.03	7.33
At1g59670	Defence/redox	ATGSTU15	9.47	7.59
At4g02520	Defence/redox	ATGSTF2	3.89	9.25
At2g02930	Defence/redox	ATGSTF3	3.81	7.69
At2g14610	Defence/redox	PR1	39.30	191.65
At2g43590	Defence/redox	Chitinase, putative	3.36	11.97
At2g43620	Defence/redox	Chitinase, putative	4.23	15.88
At2g44490	Defence/redox	PEN2 (penetration 2)	3.31	5.56
At4g14400	Defence/redox	ACD6 (accelerated cell death 6)	8.45	39.62
At5g23020	Glucosinolate metabolism	MAM-L (methylthioalkymalate synthase-like)	6.23	4.86
At1g54040	Glucosinolate metabolism	ESP (epithiospecifier protein)	15.04	11.18
At3g06910	Protein metabolism	Ulp1 protease family protein	4.90	9.20
At5g24240	Protein metabolism	Phosphatidylinositol 3, 4-kinase family protein	3.16	3.09
At1g13200	Protein metabolism	F-box family protein	3.66	5.71
At3g58880	Protein metabolism	F-box family protein	27.96	16.68
At1g28060	RNA metabolism/transcription	snRNP family protein	3.36	3.93
At1g58025	RNA metabolism/transcription	DNA binding	67.59	50.11
At4g24420	RNA metabolism/transcription	RNA recognition motif (RRM)	14.71	16.01
At2g41100	Signalling	TCH3 (Touch3)	–	4.73
At3g03950	Signalling	ECT1, protein binding	–	3.10
At3g04110	Signalling	GLR1 (glutamate receptor 1)	–	3.42
At4g23130	Signalling	CRK5 (cysteine-rich PLK5)	–	7.03
At4g23180	Signalling	CRK10 (cysteine-rich PLK10)	–	3.06
At2g19190	Signalling	FRK1 (FLG22-induced receptor-like kinase)	4.11	4.37
At1g51850	Signalling	leucine-rich repeat protein kinase	3.15	8.13
At1g21250	Signalling	WAK1 (wall-associated kinase 1)	–	5.83
At1g21270	Signalling	WAK2 (wall-associated kinase 2)	–	4.87
At5g38260	Signalling	Serine/threonine protein kinase	6.47	16.28
At4g15210	Carbon metabolism	Beta-amylase	3.69	7.23
At1g59124	Defence/redox	Disease resistance	4.43	3.03
At4g16950	Defence/redox	RPP5 (recognition of peronospora parasitica 5)	4.12	3.43
At3g46530	Defence/redox	RPP13	3.14	–
At3g50480	Defence/redox	HR4 (homolog of RPW8 4)	9.66	3.99
At1g62540	Defence/redox	Flavin-containing monooxygenase	8.38	6.81
At1g35310	Defence/redox	Bet v I allergen family protein	4.67	7.86
At5g39130	Defence/redox	Germin-like protein, putative	12.01	27.82
At4g27140	Development	2S seed storage protein 1	–	19.54
At4g27150	Development	2S seed storage protein 2	–	30.96
At4g27160	Development	2S seed storage protein 3	–	37.81
At5g44120	Development	CRA1 (Cruciferin 1)	–	49.17
At4g28520	Development	CRU3 (Cruciferin 3)	–	49.52
At5g23010	Glucosinolate metabolism	MAM1 (2-isopropylmalate synthase 3)	7.50	13.00
At2g30840	Glucosinolate metabolism	2-Oxoglutarate-dependent dioxygenase	14.00	18.44
At2g25450	Glucosinolate metabolism	2-Oxoglutarate-dependent dioxygenase	107.30	69.99
At5g25980	Glucosinolate metabolism	TGG2 (glucoside glucohydrolase 2)	40.32	38.56
At2g03710	RNA metabolism/transcription	SEP4 (Sepallata4)	5.86	7.42
At1g75290	Secondary metabolism	Isoflavone reductase, putative	–	4.40
At3g25830	Secondary metabolism	TPS-CIN (terpene synthase-like)	–	3.64
At5g44630	Secondary metabolism	Terpene synthase/cyclase family protein	–	8.65
At3g10340	Secondary metabolism	Phenylalanine ammonia-lyase, putative	–	4.29
At2g38080	Secondary metabolism	IRX12/LAC4 (laccase 4)	–	4.24
At2g34840	Transport	Coatomer protein epsilon subunit family protein	3.50	3.20
At4g13800	Transport	Permease related	3.02	3.22
At4g25950	Transport	VATG3 (vacuolar ATP synthase G3)	5.10	5.50

The entire gene list is provided in Supporting Information Table S4.
AGI, Arabidopsis Genome Initiative.

From the transcript profiles, we detected no evidence for a developmental difference between two ecotypes in 21 June. Any differences between ecotypes were mainly restricted to the categories that may be summarized as stress specific and stress defence specific (Table 3, Supporting Information Table S4). Cvi-0 highly expressed GSTs, for example, *GSTU10* and *GSTU15*, and biotic stress-related genes such as *PR1* and *PEN2* (Supporting Information Table S4A). However, Col-0 highly expressed TIR-NBS-LRR class and CC-NBS-LRR class disease resistance proteins including RPP5 and RPP13 (Supporting Information Table S4B). Not surprisingly, transcripts known to account for natural variation in glucosinolate biosynthesis (methyl-sulfinylalkyl, alkenyl and hydroxyalkyl glucosinolates) in different *Arabidopsis* ecotypes were also picked up by this comparison (Kroymann *et al.* 2003): *ESP* and *AOP3* had higher expression in Cvi-0, but *MAM1* had higher expression in Col-0. *TGG2*, related to glucosinolate catabolism, and three 2-oxoglutarate-dependent dioxygenases were highly expressed only in Col-0, which may provide additional candidates for studying the natural variation in glucosinolate metabolism.

By 27 June, *SEP4* and *STK*, preferentially expressed in ovules, and transcripts for 2S and 12S seed storage proteins were more highly expressed in Col-0 compared with Cvi-0 (Table 3, Supporting Information Table S4D), indicating that development had progressed further, or faster, in Col-0 than in Cvi-0. This is consistent with known differences in flowering time between these two ecotypes. The expression of GSTs, biotic stress and genes related to glucosinolate metabolism distinguishing the two ecotypes was still evident in functions different from development. Interestingly, 7 ankyrin repeat family proteins, including ACD6, involved in resistance to *Pseudomonas syringae*, and ANK, responding to salicylic acid, and 15 receptor kinases were highly expressed in Cvi-0 alone (Supporting Information Table S4C), while genes related to secondary metabolism-related genes were more highly expressed in Col-0 in 27 June (Supporting Information Table S4D).

Gene family analysis and display by MapMan

Members of gene families [according to The Arabidopsis Information Resource (TAIR)] related to defence/redox, transport, signalling and transcription factors are displayed as heatmaps (Fig. 2; genes are identified in Supporting Information Table S5). Both ecotypes up-regulated GSTs, peroxidases and HSPs in elevated [CO2], especially at the second harvest date. Particularly interesting, ER-type Ca-ATPases (At4g00900, *ECA2*; At1g10130, *ECA3*), PM-type Ca-ATPases (At1g27770, *ACA1*; At4g29900, *ACA10*) and a Ca^{2+}/H^+ exchanger (At5g17860, *CAX7*) increased at the first harvest date only in both ecotypes. Acidic amino acid permease (AAAP)-type amino acid transporters and functionally unknown endosome-located proteins were also significantly up-regulated at an earlier time in both ecotypes. This first harvest date also indicated an increased participation of MAPK signalling pathways
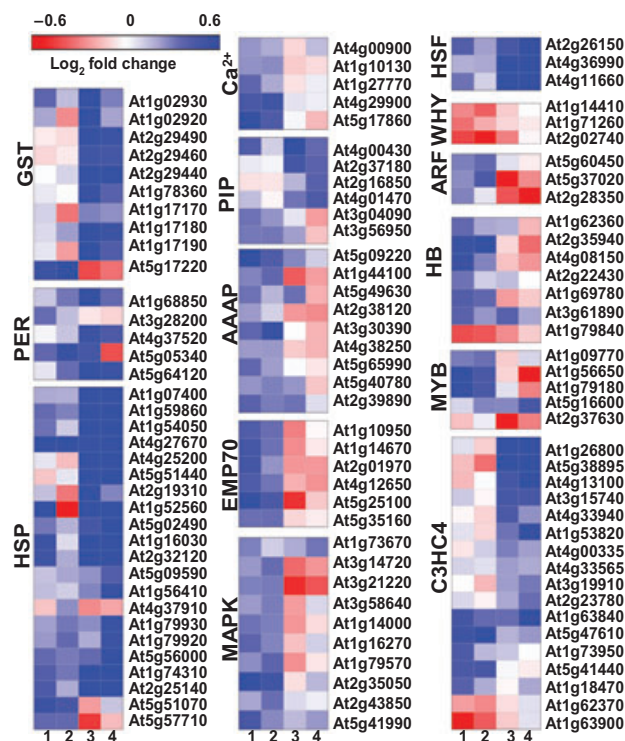

Figure 2. Heat map of transcripts in selected gene families. Significant $\log_2$ expression changes in elevated [CO2] versus ambient air were used. Up-regulation (blue colour), down-regulation (red) and no change (white) are indicated. (1) Col-0 (June 21), (2) Cvi-0 (June 21), (3) Col-0 (June 27) and (4) Cvi-0 (June 27).

with coordinated up-regulation of MAPKs, MAPKKs and MAPKKKs. Elevated [CO2] repressed family members of Whirly transcription factors at the first harvest date, however, increased the expression of, for example, ARFs that later declined. Consistent with HSPs, heat stress transcription factors (HSFs) were also increased in elevated [CO2].

MapMan software was used to investigate pathways influenced by elevated [CO2] in each ecotype and time point (Supporting Information Fig. S4A–C). The Wilcoxon test was used to identify categories whose member genes showed a statistically significant coordinated response compared with the response of other genes included on the array. The *P*-values were calculated for elevated [CO2] versus ambient [CO2], and are included in the Supporting Information Table S5-2. Consistent with the ANOVA results, growth at elevated [CO2] repressed the expression of photosynthetic genes and stimulated the expression of genes in pathways consuming carbon, exemplified by enhanced cell wall biosynthesis (21 June). However, transcripts for cytosolic ribosomal proteins displayed a different response to elevated [CO2], being consistently down-regulated in Col-0, while they were only minimally regulated in Cvi-0. In contrast, by 27 June, Cvi-0 appeared to have adjusted, while Col-0 began to show signs of senescence, exemplified by further down-regulation of photosynthesis functions and chloroplast

ribosomal proteins. It is noteworthy to realize that Cvi-0, showing much less of a phenotype that appears to indicate a disturbance of the C : N ratio (Fig. 5) at this time, had only started to enter flowering, while Col-0 had largely terminated flowering but still showed the disturbance (Fig. 5).

Integration of metabolite and transcript profiles

The analysis of metabolites in both ecotypes collected at both time points focused on abundant metabolites (Supporting Information Table S6). Obvious changes identified sugars in general; glucose, galactose and maltose increased significantly in elevated [CO_2] at all times in both ecotypes, while increases in fructose and raffinose were less pronounced or restricted to Col-0. No significant changes were observed for sucrose (Fig. 3). Most amino acid showed decreases in elevated CO_2 except for histidine, tryptophan and phenylanine, the increases likely indicating flux into

pathways of secondary metabolism. There was an obvious difference between ecotypes in glutamic acid and glutamine at the second harvest day: both declined precipitously in Col-0, but increased (glutamic acid) or maintained the level observed in ambient air (glutamine) in Cvi-0. However, among organic acids, isocitrate and malic acid were exceptionally high, and malic acid increased in elevated [CO_2] at all times in both ecotypes. At the second harvest date, succinic acid also had increased in both ecotypes (Fig. 3).

The high levels of hexoses could provide substrates for glycolysis, and the large increases in TCA cycle intermediates indeed supported a view of increased C-partitioning to respiration or for anabolic pathways originating from the mitochondrial and cytosolic compartments. Figure 3 (Supporting Information Table S7) integrates these major metabolites with transcript profiles. Placed next to enzyme i.d.s in pathways of primary metabolism symbols for up- or down-regulation, no change or missing data are included
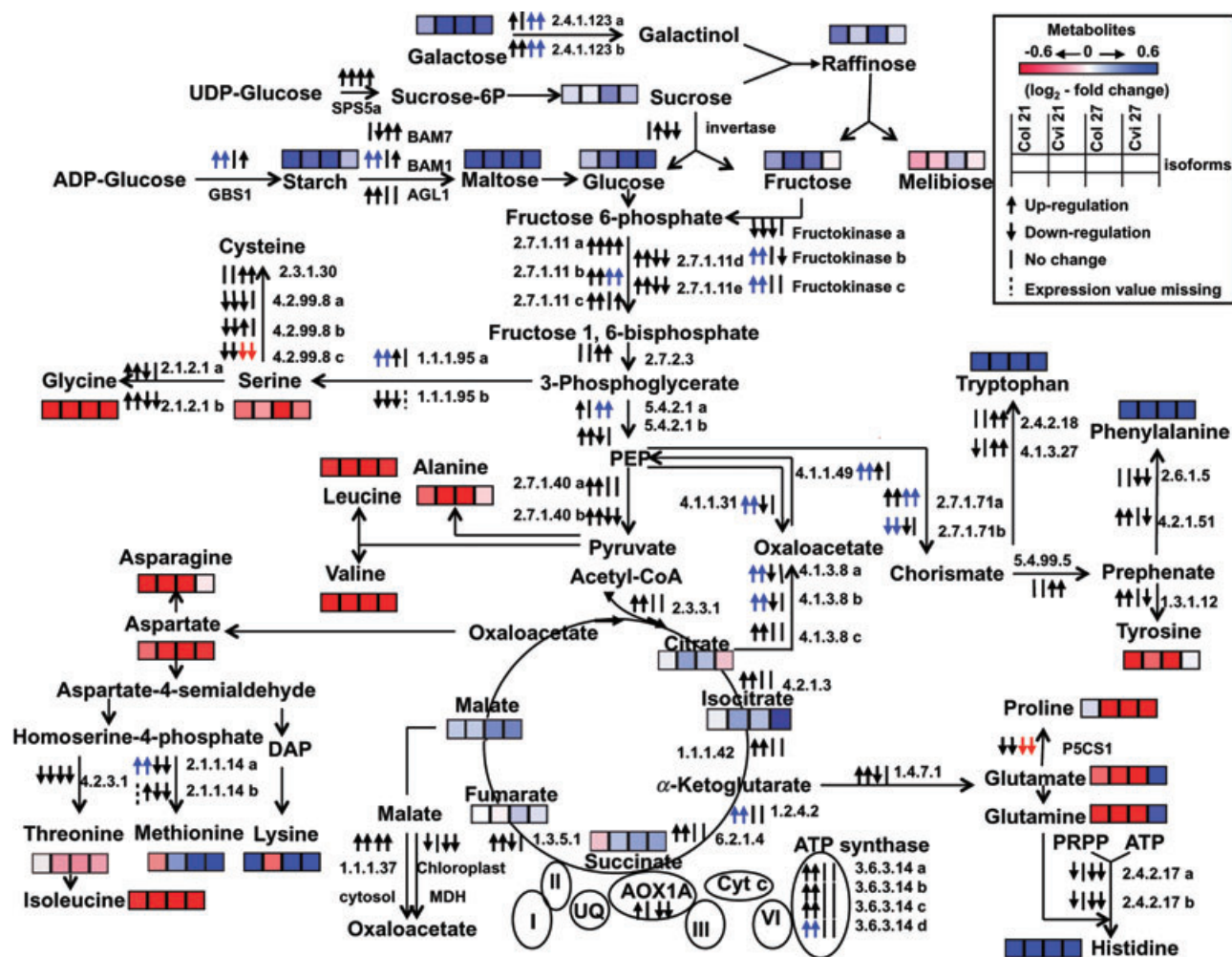

Figure 3. Overview of transcript and metabolite changes in pathways of primary carbohydrate and amino acid metabolism. Changes in transcript expression and metabolites in Col-0 and Cvi-0 (21 and 27 June 2005). Blue or red blocks indicate increases or decreases of metabolites, respectively. Regulation of transcripts is indicated by the direction of the arrows. Blue or red arrows indicate a significant up- or down-regulation (adjusted $P < 0.05$); black arrows indicate an insignificant trend, and no change (bar) or no data (stippled bar) are included. Values for Col-0 (21 June), Cvi-0 (21 June), Col-0 (27 June) and Cvi-0 (27 June) are compared from left to right.
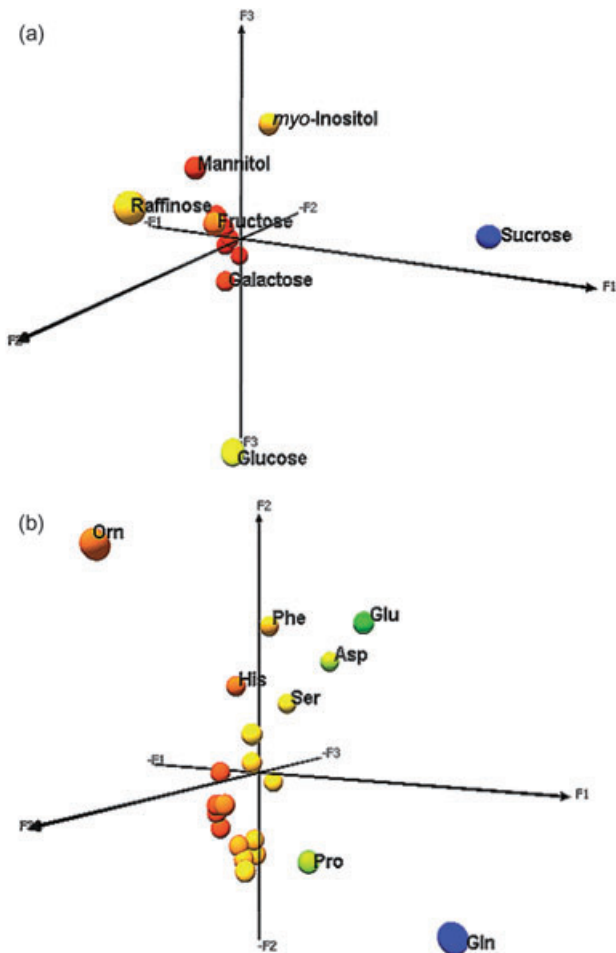
Figure 4. Principal component analysis of metabolites. Sugars and sugar alcohols (a) and amino acids (b) at the second harvest date are shown. Components in (a) are F1 (ecotype-specific differences): sucrose; F2 (time of harvest): raffinose, glucose, sucrose, maltose and fructose; and F3 ([CO$_2$] versus ambient): glucose, *myo*-inositol, mannitol, raffinose and galactose. Components in (b) are F1 ([CO$_2$] versus ambient): glutamine and glutamic acid; F2 ([CO$_2$] versus ambient): ornithine, glutamic acid, lysine, histidine and phenylalanine; F3 (ecotype-specific): glutamine, glutamic acid, proline, ornithine and aspartic acid.

for all isoforms that could be scored at both harvest dates. The transcript profiles indicated active engagement of glycolysis and the TCA cycle at the first harvest date only. However, the increase of C skeletons did not result in the accumulation of most amino acids. Furthermore, transcripts related to amino acid biosynthesis were down-regulated or did not change, with the exception of those involved in tryptophan and phenylalanine biosynthesis.

Figure 4 presents statistical data in the form of the PCA of the metabolite profiling experiments. When all metabolites, times of harvest, treatment and ecotypes were included, the major component identified the CO$_2$ effect, followed by the time of harvest and ecotypic different behaviour (not shown). When focusing on sugars and polyols (Fig. 4a), sucrose content distinguished the ecotypes (F1), while harvest date and [CO$_2$] effect contributed less.

Amino acid composition (Fig. 4b) revealed the importance of the [CO$_2$] effect (F1 and F2), while ecotype differences were less important (F3).

The accumulation of organic acids, decline in amino acid amounts and disparate regulation of genes in glycolysis/TCA and amino acid metabolism suggested a metabolic perturbation at the interface of C and N utilization. An experiment that monitored *Arabidopsis* (Col-0) transcript profiles in nitrogen deficiency (Usadel *et al.* 2005) had identified a number of genes that showed an up- or down-regulation. Many of these N deficiency-related genes were also regulated in this FACE experiment (Fig. 5; genes are identified in Supporting Information Table S8). In fact, at the first harvest date, most transcripts that down-regulated during an experimentally induced N deficiency were also down-regulated in Col-0 and Cvi-0 after exposed to the elevated CO$_2$, and many up-regulated genes were also regulated in common. The correlation in gene expression changes between N deficiency and elevated [CO$_2$] persisted for Col-0 at the second harvest date, while Cvi-0 did not exhibit the same pattern. The contrast between Col-0 and Cvi-0 exemplifies differences in how both ecotypes adjusted to changes in the C : N ratio, which appear to accompany their growth in elevated [CO$_2$], equally indicating the existence of genetic diversity to changes in the composition of the atmosphere.

DISCUSSION

In a comparison of transcript profiles in three *Arabidopsis* ecotypes, many chloroplast functions decreased in elevated
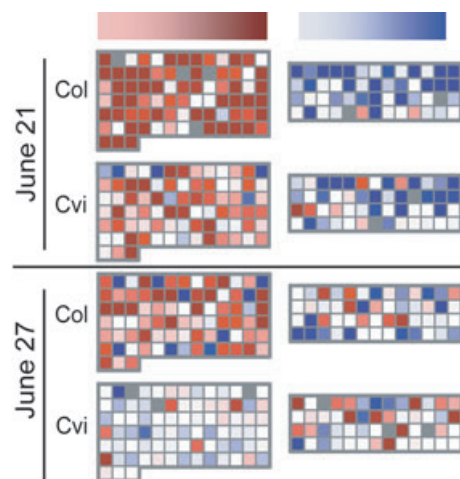

Figure 5. Comparison of N-deficiency responses with responses by *Arabidopsis* ecotypes in elevated [CO$_2$]. Regulated transcripts in Free-Air CO$_2$ Enrichment (FACE) are compared with transcript changes observed during nitrogen starvation (Usadel *et al.* 2005). Up-regulation is indicated by shades of blue, down-regulation by red. In cases where a similar response is encountered, the individual spots in an area show the same colour as the guide bars. Up- and down-regulated transcripts (log$_2$ scale, +0.5 to −0.5) are identified by *Arabidopsis* i.d. and annotation in Supporting Information Table S8. The analysis indicated Col-0 showing a stronger N-deficiency response than Cvi-0.

[CO$_2$], in particular transcripts in photosynthesis and CO$_2$ fixation (Li *et al.* 2006). In comparison with ambient air, increased transcriptional activity characterized hexose utilization, starch turnover, cell wall biosynthesis and, to a smaller degree, secondary metabolism. Similar results obtained in FACE experiments and in growth chambers have been reported, and our results in this earlier study showed an overall correlation. Furthermore, this study conducted in 2003 revealed a subset of transcripts that behaved identically in all ecotypes, identifying genes that also regulated under nitrogen-deficiency conditions (Li *et al.* 2006). The majority of these genes has also been identified in the present study at the first harvest day (21 June 2005), which regulated the same way. At the second harvest date (27 June 2005), at much higher temperatures, the correlation was less pronounced, indicating how local weather was reflected in these profiles. The overlapping transcripts between the two harvest dates also indicated a strong influence of weather and development. In the comparison of ambient versus CO$_2$-enriched air, *Arabidopsis* ecotypes nonetheless responded to local weather conditions with differences in their capacity to acclimate.

Focusing on ecotypes Col-0 and Cvi-0, their adaptation to distinctly different habitats, time of analysis, weather and the comparison of elevated [CO$_2$] with ambient air provided insights that identified the likely obstacles for C$_3$ plants to make an optimal use of elevated CO$_2$. Both ecotypes grew well in SoyFACE, while growth, flowering time and seed set showed ecotype-specific variation, which was, however, not influenced by CO$_2$, but rather by field conditions that accelerated growth and development as reported before (Miyazaki *et al.* 2004; Li *et al.* 2006). The selection of the two *Arabidopsis* ecotypes was based on a divergent response to the [CO$_2$] environment. Natural genetic variation that controls phenotypic differences are well documented in *Arabidopsis*, with examples such as flowering time (Chen *et al.* 2005), ecotype-specific expression of duplicated genes (Clauss & Mitchell-Olds 2004), glucosinolate biosynthesis (Kliebenstein *et al.* 2001), pathogen susceptibility (Bidart-Bouzat, Mithen & Berenbaum 2005) or oxidative stress tolerance (Tamaoki *et al.* 2003). We further reasoned that the plant's short life span, growing in multiple FACE plots in sufficient number for repeat samplings, would provide snapshots about how the plants responded to elevated [CO$_2$] and how this would be reflected by changes in gene expression and metabolites. Our physiological analyses correlated well with those of other FACE experiments (Davey *et al.* 2004; Horz *et al.* 2004; Long *et al.* 2004, 2005; Morgan *et al.* 2004; Ainsworth & Long 2005; Tricker *et al.* 2005; Reich *et al.* 2006). The ecotypic differences in transcript behaviour then suggested mechanisms that begin to explain the less-than-expected use of elevated [CO$_2$] by C$_3$ plants, clearly indicating that genetic diversity exists, which might not be obvious or exploited in extant crops.

Expression profiles and metabolites grouped in a way that first separated the two harvest dates and reflected the microclimate difference between the time points. A surprisingly strong change was revealed in the transcription profiles, ambient versus elevated [CO$_2$], with respect to cellular compartments and functional categories affected (Table 2, Supporting Information Table S3). Chloroplast-localized transcripts unrelated to light capture and fixation functions declined strongly and mostly remained repressed. Many transcripts in secretory pathways were up-regulated early, and many remained high throughout the experiment. Transcripts located in mitochondria increased especially at later times. This reflected the increased importance of investment in the metabolic machinery utilizing increased carbon versus prioritization of carbon fixation as a limiting factor in ambient [CO$_2$]. Declines were always more pronounced in Col-0, while Cvi-0 recovered over time to begin to resemble plants growing in ambient air. In terms of functional categories, apart from the well-known up-regulated categories (carbon, cell wall and secondary metabolism), lipid metabolism, signalling and transport functions increased early during the plants' growth in elevated [CO$_2$], but functions in protein metabolism and defence dominated among the up-regulated transcripts later.

The behaviour of the *Arabidopsis* transcriptome under nutrient deficit modelled into the MapMan program (Usadel *et al.* 2005) provided what might be the most coherent insight. Figure 5 compares data from SoyFACE with previously recorded gene expression changes by plants in low N (Usadel *et al.* 2005). We inserted the regulatory changes observed in our experiments for the genes altered by nitrogen deficiency to generate response-similarity maps (Supporting Information Table S8 for gene i.d.s). Col-0 at both harvest dates showed up- and down-regulations that were largely identical to those observed under N-deficiency conditions (and to some degree, also P deficit; data not shown). Cvi-0 showed this pattern very clearly at the early harvest date, but not at the second. Genes in categories reactive oxygen species (ROS), secondary metabolism, chaperone activities, as well as genes that down-regulate carbon fixation in the absence of nitrogen, were expressed similarly in both N deficiency and elevated [CO$_2$] (Supporting Information Table S8). Increased photosynthetic [CO$_2$] fixation altered the apparent C/N balance to which the two ecotypes responded differently.

The imbalance seemed to constrain the benefits arising from the growth in elevated [CO$_2$], also indicated by the dramatic increases of transcripts for HSPs and GSTs (Fig. 2). The imbalance in C : N metabolism, signalling an apparent decline in nitrogen, seems to be one main driver for changes in gene expression and metabolism. However, these changes are not to be confused with what is typically viewed as plant biotic or abiotic stress responses. This view is supported by a comparison of Col-0 plants grown in the greenhouse, with plants grown in ambient air in FACE (Miyazaki *et al.* 2004). A large number among the genes with significant changes in transcript amount identified stress-associated functions in ambient air in the field. Elevated [CO$_2$] further increased transcripts in defence, ROS and chaperone categories. Among the ecotypes here, significant differences identified the categories defence and redox homeostasis, exemplified by PR1 and RPP5, and

proteins related to ROS scavenging such as GST. Metabolite analyses provided similar trends in as far as pathways that consume or store carbon were most significantly increased, including several organic acids in the TCA cycle, mirroring the behaviour of transcripts for glycolysis and TCA cycle enzymes. Paradoxically, the increase in substrates for transaminations did not result in increased amino acid accumulation with the exception of increased levels of aromatic amino acids.

The *Arabidopsis* ecotypes were not able to capitalize from the benefits of elevated [CO$_2$] as much as might be expected. Perception of increased concentrations of some C compounds could be at the basis of this molecular response, with sugar sensing then resulting in the down-regulation of metabolism, unless, as in N-fixing species, additional N compounds could be provided, or unless, as in trees, a large sink was available to accommodate excess C. This view might explain the discrepancy between expected and real gains in elevated [CO$_2$] (Ainsworth & Long 2005). The correspondence between our results and the physiological observations in other species supports the use of the *Arabidopsis* model as a tool for uncovering the molecular genetic mechanisms that prevent plants from realizing the advantages that could potentially be provided by elevated [CO$_2$]. Based on the resources and databases in this model, unparalleled among plants, it should be possible to analyse the veracity of the information gained in species of economic significance.

ACKNOWLEDGMENTS

REFERENCES

Ainsworth E.A. & Long S.P. (2005) What have we learned from 15 years of free-air CO$_2$ enrichment (FACE)? A meta-analytic review of the responses of photosynthesis, canopy properties and plant production to rising CO$_2$. *New Phytologist* **165**, 351–371.

Ainsworth E.A. & Rogers A. (2007) The response of photosynthesis and stomatal conductance to rising [CO$_2$]: mechanisms and environmental interactions. *Plant, Cell & Environment* **30**, 258–270.

Ainsworth E.A., Rogers A., Vodkin L.O., Walter A. & Schurr U. (2006) The effects of elevated CO$_2$ concentration on soybean gene expression. An analysis of growing and mature leaves. *Plant Physiology* **142**, 135–147.

Ainsworth E.A., Rogers A., Leakey A.D., Heady L.E., Gibon Y., Stitt M. & Schurr U. (2007) Does elevated atmospheric [CO$_2$] alter diurnal C uptake and the balance of C and N metabolites in growing and fully expanded soybean leaves? *Journal of Experimental Botany* **58**, 579–591.

Bazzaz F.A., Jasienski M., Thomas S.C. & Wayne P. (1995) Micro-evolutionary responses in experimental populations of plants to CO$_2$-enriched environments: parallel results from two model systems. *Proceedings of the National Academy of Sciences of the United States of America* **92**, 8161–8165.

Bidart-Bouzat M.G., Mithen R. & Berenbaum M.R. (2005) Elevated CO$_2$ influences herbivory-induced defense responses of *Arabidopsis thaliana*. *Oecologia* **145**, 415–424.

Castells E., Roumet C., Peñuelas J. & Roy J. (2002) Intraspecific variability of phenolic compounds and their responses to elevated CO$_2$ in two Mediterranean perennial grasses. *Environmental and Experimental Botany* **47**, 205–216.

Chen W., Chang S., Hudson M., Kwan W., Li J., Estes B., Knoll D., Shi L. & Zhu T. (2005) Contribution of transcriptional regulation to natural variations in *Arabidopsis*. *Genome Biology* **6**, R32.

Cheng S.H., Moore B.D. & Seemann J.R. (1998) Effects of short- and long-term elevated CO$_2$ on the expression of ribulose-1,5-bisphosphate carboxylase/oxygenase genes and carbohydrate accumulation in leaves of *Arabidopsis thaliana* (L.) Heynh.1. *Plant Physiology* **116**, 715–723.

Clauss M.J. & Mitchell-Olds T. (2004) Functional divergence in tandemly duplicated *Arabidopsis thaliana* trypsin inhibitor genes. *Genetics* **166**, 1419–1436.

Cui X., Hwang J.T., Qiu J., Blades N.J. & Churchill G.A. (2005) Improved statistical tests for differential gene expression by shrinking variance components estimates. *Biostatistics* **6**, 59–75.

Davey P.A., Hunt S., Hymus G.J., DeLucia E.H., Drake B.G., Karnosky D.F. & Long S.P. (2004) Respiratory oxygen uptake is not decreased by an instantaneous elevation of [CO$_2$], but is increased with long-term growth in the field at elevated [CO$_2$]. *Plant Physiology* **134**, 520–527.

Duarte J.M., Cui L., Wall P.K., Zhang Q., Zhang X., Leebens-Mack J., Ma H., Altman N. & Depamphilis C.W. (2006) Expression pattern shifts following duplication indicative of subfunctionalization and neofunctionalization in regulatory genes of *Arabidopsis*. *Molecular Biology and Evolution* **23**, 469–478.

Gong Q., Li P., Ma S., Rupassara S.I. & Bohnert H.J. (2005) Stress adaptation competence in *Arabidopsis thaliana* and its extremophile relative *Thellungiella halophila*. *The Plant Journal* **44**, 826–839.

Gupta P., Duplessis S., White H., Karnosky D.F., Martin F. & Podila G.K. (2005) Gene expression patterns of trembling aspen trees following long-term exposure to interacting elevated CO$_2$ and tropospheric O$_3$. *New Phytologist* **167**, 129–142.

Horz H.P., Barbrook A., Field C.B. & Bohannan B.J. (2004) Ammonia-oxidizing bacteria respond to multifactorial global change. *Proceedings of the National Academy of Sciences of the United States of America* **101**, 15136–15141.

Jaakola L., Pirttila A.M., Halonen M. & Hohtola A. (2001) Isolation of high quality RNA from bilberry (*Vaccinium myrtillus* L.) fruit. *Molecular Biotechnology* **19**, 210–203.

Jobson J.D. (1992) *Applied Multivariate Data Analysis. Volume: II: Categorical and Multivariate Methods*, pp. 483–568. Springer-Verlag, New York, NY, USA.

Jolliffe I.T. (2002) *Principal Component Analysis*, 2nd edn. Springer, New York, NY, USA.

Kliebenstein D.J., Kroymann J., Brown P., Figuth A., Pedersen D., Gershenzon J. & Mitchell-Olds T. (2001) Genetic control of natural variation in *Arabidopsis* glucosinolate accumulation. *Plant Physiology* **126**, 811–825.

Kroymann J., Donnerhacke S., Schnabelrauch D. & Mitchell-Olds T. (2003) Evolutionary dynamics of an Arabidopsis insect resistance quantitative trait locus. *Proceedings of the National Academy of Sciences of the United States of America* **100**, 14587–14592.

Li P., Sioson A.A., Mane S.P., Ulanov A., Grothaus G., Heath L.S., Murali T.M., Bohnert H.J. & Grene R. (2006) Response diversity

of *Arabidopsis thaliana* ecotypes in elevated CO₂ in the field. *Plant Molecular Biology* **62,** 593–609.

Long S.P., Ainsworth E.A., Rogers A. & Ort D.R. (2004) Rising atmospheric carbon dioxide: plants FACE the future. *Annual Review of Plant Biology* **55,** 591–628.

Long S.P., Ainsworth E.A., Leakey A.D.B. & Morgan P.B. (2005) Global food insecurity. Treatment of major food crops with elevated carbon dioxide or ozone under large-scale fully open-air conditions suggests recent models may have overestimated future yield. *Transactions of the Royal Society of London* **360,** 2011–2020.

Lozovaya V., Ulanov A., Lygin A., Duncan D. & Widholm J. (2006) Biochemical features of maize tissues with different capacities to regenerate plants. *Planta* **224,** 1385–1399.

Ludewig F., Sonnewald U., Kauder F., Heineke D., Geiger M., Stitt M., Muller-Röber B.T., Gillissen B., Kuhn C. & Frommer W.B. (1998) The role of transient starch in acclimation to elevated atmospheric CO₂. *FEBS Letters* **429,** 147–151.

Miyazaki S., Fredricksen M., Hollis K.C., Poroyko V., Shepley D., Galbraith D.W., Long S.P. & Bohnert H.J. (2004) Expression profiles for *Arabidopsis thaliana* grown at UIUC SoyFACE. *Field Crops Research* **90,** 47–59.

Morgan P.B., Bernacchi C.J., Ort D.R. & Long S.P. (2004) An in vivo analysis of the effect of season-long open-air elevation of ozone to anticipated 2050 levels on photosynthesis in soybean. *Plant Physiology* **135,** 2348–2357.

Peñuelas J. & Estiarte M. (1998) Can elevated CO₂ affect secondary metabolism and ecosystem function? *Trends in Ecology and Evolution* **13,** 20–24.

Porra R.J., Thompson W.A. & Kriedemann P.E. (1989) Determination of accurate extinction coefficients and simultaneous-equations for assaying chlorophyll-a and chlorophyll-b extracted with 4 different solvents – verification of the concentration of chlorophyll standards by atomic-absorption spectroscopy. *Biochimica et Biophysica Acta* **975,** 384–394.

Prentice I.C., Farquhar G.D., Fasham M., Goulden M., Jaramillo V., Kheshgi H., Quere C., Scholes R. & Wallace D. (2001) The carbon cycle and atmospheric CO2. In *Climate Change 2001: The Scientific Basis. Contribution of Working Group 1 to the Third Assessment Report of the Intergovernmental Panel on Climate Change* (eds J.T. Houghton, Y.D. Ding, J. Griggs, M. Noguer, P.J. van der Linden, X. Dai, K. Maskell & C.A. Johnson), pp. 183–237. Cambridge University Press, Cambridge, UK.

Reich P.B., Tjoelker M.G., Machado J.L. & Oleksyn J. (2006) Universal scaling of respiratory metabolism, size and nitrogen in plants. *Nature* **439,** 457–461.

Roessner U., Wagner C., Kopka J., Trethewey R.N. & Willmitzer L. (2000) Simultaneous analysis of metabolites in potato tuber by gas chromatography-mass spectrometry. *The Plant Journal* **23,** 131–142.

Silva B.M., Casal S., Andrade P.B., Seabra R.M., Oliveira M.B. & Ferreira M.A. (2003) Development and evaluation of a GC/FID method for the analysis of free amino acids in quince fruit and jam. *Analytical Science* **19,** 1285–1290.

Stitt M., Lilley R.M., Gerhardt R. & Heldt H.W. (1989) Metabolite levels in specific cells and subcellular compartments of plant leaves. *Method in Enzymol* **174,** 518–552.

Tamaoki M., Matsuyama T., Kanna M., Nakajima N., Kubo A., Aono M. & Saji H. (2003) Differential ozone sensitivity among *Arabidopsis* accessions and its relevance to ethylene synthesis. *Planta* **216,** 552–560.

Taylor G., Street N.R., Tricker P.J., Sjödin A., Graham L., Skogström O., Calfapietra C., Scarascia-Mugnozza G. & Jansson S. (2005) The transcriptome of Populus in elevated CO₂. *New Phytologist* **167,** 143–154.

Thimm O., Blasing O., Gibon Y., Nagel A., Meyer S., Kruger P., Selbig J., Muller L.A., Rhee S.Y. & Stitt M. (2004) MAPMAN: a user-driven tool to display genomics data sets onto diagrams of metabolic pathways and other biological processes. *The Plant Journal* **37,** 914–939.

Tricker P.J., Trewin H., Kull O., Clarkson G.J., Eensalu E., Tallis M.J., Colella A., Doncaster C.P., Sabatti M. & Taylor G. (2005) Stomatal conductance and not stomatal density determines the long-term reduction in leaf transpiration of poplar in elevated CO₂. *Oecologia* **143,** 652–660.

Usadel B., Nagel A., Thimm O., *et al.* (2005) Extension of the visualization tool MapMan to allow statistical analysis of arrays, display of corresponding genes, and comparison with known responses. *Plant Physiology* **138,** 1195–1204.

SUPPORTING INFORMATION

Additional Supporting Information may be found in the online version of this article:

Figure S1. Chlorophyll (A) and protein (B) content of leaves of Col-0 and Cvi-0 harvested on June 21 and June 27, 2005, respectively. Data represent the mean (±SD) from three rings (5 repeats per ring, and 10 plants pooled in each ring repeat).

Figure S2. Hierarchical clustering over all experimental conditions. Genes (11 758) that passed normalization and low-intensity filtering in all slides were clustered using hierarchical clustering (UPGMA, unweighted average with the similarity measure based on Euclidean distance). Ordering function was based on average value. The dendrogram is based on similarity between profiles. Down-regulation (red), up-regulation (blue) and no change (white).

Figure S3. Verification of microarray results by real-time PCR. Log₂ (elevated CO₂/ambient) values for genes (a–n) in the four experimental conditions. Genes: (a) *At3g51240,* (b) *At1g61800,* (c) *At2g31390,* (d) *At1g02930,* (e) *At2g37040,* (f) *At3g09640,* (g) *At3g59700,* (h) *At4g09010,* (i) *At4g16150,* (j) *At4g25080,* (k) *At4g31870,* (l) *At4g34190,* (m) *At5g15490* and (n) *At5g63310.* The primers were listed in the Supporting Information Table S2.

Figure S4. MapMan images for categories photosynthesis (A), cell wall precursors (B) and ribosomal proteins and translation (C). (SF4A-1) Photosynthesis of Col-0 at June 21; (SF4A-2) photosynthesis of Cvi-0 at June 21; (SF4A-3) photosynthesis of Col-0 at June 27; (SF4A-4) photosynthesis of Cvi-0 at June 27. (SF4B-1) Cell wall precursor of Col-0 at June 21; (SF4B-2) cell wall precursor of Cvi-0 at June 21; (SF4B-3) cell wall precursor of Col-0 at June 27; (SF4B-4) cell wall precursor of Cvi-0 at June 27. (SF4C-1) RNA metabolism/protein synthesis of Col-0 at June 21; (SF4C-2) RNA metabolism/protein synthesis of Cvi-0 at June 21; (SF4C-3) RNA metabolism/protein synthesis of Col-0 at June 27; (SF4C-4) RNA metabolism/protein synthesis of Cvi-0 at June 27.

Table S1. Weather condition and Pearson correlation. (A) Weather conditions during sampling and the 24 h prior to

sampling. (B) Person correlation coefficient of the transcriptome among experiments.

Table S2. List of primer sequences used in RT-PCR analysis and the RT-PCR data.

Table S3. Mixed-model ANOVA identified transcripts regulated in the same direction in *Arabidopsis* ecotypes Col-0 and Cvi-0 in elevated $[CO_2]$ (FDR-adjusted $P < 0.05$). Functional distribution and protein localization prediction of the transcripts are included. (A) Down-regulated genes in June 21 in both Col-0 and Cvi-0; (B) up-regulated genes in June 21 in both Col-0 and Cvi-0; (C) down-regulated genes in June 27 in both Col-0 and Cvi-0; (D) up-regulated genes in June 27 in both Col-0 and Cvi-0.

Table S4. Mixed-model ANOVA identified genes with variation between Col-0 and Cvi-0 (FDR-adjusted $P < 0.05$).

Table S5. (1) Gene family analysis under the elevated CO_2; (2) Wilcoxon rank-sum test of MapMan categories.

Table S6. List of metabolite data.

Table S7. List of transcriptome and metabolome changes in major carbohydrate and amino acid metabolism presented in Fig. 4.

Table S8. List of all transcripts in Fig. 3 (nutrient-deficit similarity comparison).

Supporting Information text – MIAME compliance.

Please note: Wiley-Blackwell are not responsible for the content or functionality of any supporting materials supplied by the authors. Any queries (other than missing material) should be directed to the corresponding author for the article.